



Micromechanics of granular materials

## Effect of the grain elongation on the behaviour of granular materials in biaxial compression

*Influence de l'allongement des grains sur le comportement des matériaux granulaires au cours d'une compression biaxiale*

Cécile Nouguier-Lehon

Université de Lyon, École centrale de Lyon, LTDS UMR 5513, 36, avenue Guy-de-Collongue, 69134 Écully cedex, France

### ARTICLE INFO

*Article history:*

Available online 23 October 2010

*Keywords:*

Granular media  
Particle shape  
Biaxial test  
Rotations

*Mots-clés:*

Milieux granulaires  
Forme des particules  
Essai biaxial  
Rotations

### ABSTRACT

In this article we study the effect of the grain elongation on the shearing behaviour of dense granular materials by means of 2D numerical simulations of biaxial compression tests, using the *Contact Dynamics* method. The case of grains with hexagonal shapes (and four possible different elongations) is studied in comparison to the case of a sample with circular grains. For the shapes studied, samples with polygonal grains exhibit initial densities higher than the sample with discs, and the initial density decreases when the grain elongation increases. The friction angle at the residual state increases linearly with the particle elongation ratio. The cumulative rotations of discs are higher than those of polygons. Finally, in the case of elongated hexagons, the grains with highest rotations are located along thin bands because the shear bands are thinner and more persistent for these shapes.

© 2010 Académie des sciences. Published by Elsevier Masson SAS. All rights reserved.

### RÉSUMÉ

Nous étudions dans cet article l'influence de l'allongement des grains sur le comportement de matériaux granulaires denses grâce à des simulations numériques 2D de l'essai de compression biaxiale par la méthode *Contact Dynamics*. Les grains sont de forme hexagonale (et de quatre élongations différentes) et leur comportement est comparé au cas des grains circulaires. Pour les formes étudiées, les échantillons de grains polygonaux sont initialement plus denses que l'échantillon de disques, et on observe une diminution de la densité initiale quand l'allongement des grains augmente. L'angle de frottement à l'état résiduel augmente linéairement avec l'allongement des particules. La rotation cumulée des disques est beaucoup plus importante que celle des polygones. Enfin, on peut remarquer que pour ces hexagones allongés, les grains qui tournent beaucoup sont situés le long de fines bandes car pour ces formes, les bandes de cisaillement sont plus fines et moins fluctuantes.

© 2010 Académie des sciences. Published by Elsevier Masson SAS. All rights reserved.

E-mail address: [cecile.nouguier@ec-lyon.fr](mailto:cecile.nouguier@ec-lyon.fr).

## 1. Introduction

The discrete element method (DEM) has been widely used since the last thirty years to improve the understanding of physical phenomena controlling the behaviour of granular materials. It allows one to access to the microstructural parameters such as contact forces between particles, that are difficult to experimentally measure. The majority of simulations were initially performed on samples of either discs in 2D or spheres in 3D (we can cite [1–6] among others). However, it is well known that the particle shape is a characteristic that has a great influence on the behaviour of such media [7–10]. Indeed, the possibility that grains are in contact through multiple contact points (due to roughness, angularity or nonconvexity of the particles) and the eventual grain elongation modify the behaviour of these materials. Several image analyses' techniques and 3D surface reconstructions are nowadays available, that can be used in order to catch with remarkable precision the actual grain shape. However, the real shape of particles may be very complex and it is important to reproduce, in a rather simple way in numerical simulations, the main features of particle non-sphericity.

More recently, many numerical simulations were performed in order to study the effect of particle shape [11–13]. For instance, Mirghasemi et al. [14] performed numerical simulations with samples composed of 500 regular polygons (from triangles and squares to polygons with 11 edges) showing that samples made of angular particles are denser than samples with rounded particles. Az ema et al. [15] showed that the existence of face-to-face contacts in a sample made of pentagonal particles leads to a higher anisotropy for the force transmission (with strong force chains essentially carried by face-to-face contacts). In previous works, [16,17], we analysed the behaviour of samples composed of different grain shapes (circular, isotropic and anisotropic polygonal shapes). Our results clearly show the existence of a steady state of void ratio, of the shear strength and texture anisotropy, whatever the grain shape, as that has been found again by [18] from shear test simulations with samples of convex polygons. The effect of induced anisotropy was also studied by Alonso-Marroqu in et al. [19] analysing the behaviour of polygons with adjusted shapes to model the behaviour of the marble.

In the present study, we analyse the effect of particle elongation, by performing 2D numerical simulations of the biaxial compression test and using samples made of irregular hexagons with different aspect ratios. A sample of discs was also generated in order to compare with the behaviour of circular particles. First we present the numerical program and the specimen preparation. Then we analyse the effect of grain elongation on the initial state and on the global and local mechanical behaviours.

## 2. Numerical procedures

### 2.1. Numerical method

The programs used for these simulations are based on the *Contact Dynamics* (CD) method [20–23], i.e. a discrete element method that allows to model granular assemblies as a collection of rigid or deformable bodies in contact with dry friction, without the introduction of elasticity at contacts (cf. *smooth DEM* [24]). In the CD method, the impenetrability condition and the friction law are treated by using the non-smooth relations of Signorini and Coulomb, which link the relative velocity at the contact impulsion. To take the collisions into account, normal and tangential coefficients of restitution are introduced, respectively denoted  $e_N$  and  $e_T$ , with values between 0 and 1. Pure elastic shocks are considered for  $e_N = e_T = 1$ , while the entire energy vanishes during impact for  $e_N = e_T = 0$ . Finally, the equations of motion are discretized by an implicit algorithm, that allows to choose larger time steps than the smooth DEM. The CD method has been used in very various fields from Civil Engineering to Biomechanics: among others we can cite the modelling of the ballast behaviour [25] and of rock avalanches [26], the study of masonry structures [27], or the analyse of cytoskeleton structuration [28]. Comparisons between simulations performed with the CD method and smooth DEM showed that both numerical methods give similar results for quasistatic tests [29,30].

### 2.2. Shape characterisation and sample generation

The particle elongation [31] can be defined as the ratio  $\frac{b}{a}$ , where  $a$  is the diameter of the smallest circle containing the particle and  $b$  is the diameter of the largest circle included in the particle (Fig. 1). So the elongation ratio  $\frac{b}{a}$  is the inverse of the aspect ratio, a parameter also used to characterise the particle elongation, that is defined as the ratio of the largest particle size to the smallest one. For a circular particle,  $\frac{b}{a} = 1$  and the higher the particle elongation the smaller the ratio  $\frac{b}{a}$ .

Starting from the same particle size distribution ( $d_{min} = 0.66$  cm,  $d_{max} = 2$  cm and a uniform distribution in particle surface fraction), the polygons are generated in order to obtain particles having, for a given diameter, the most elongated shape. To avoid the effect of particle roundness, all the polygonal shapes have six edges. The two first vertices are put diametrically opposed on the circle of  $a$  in diameter (points  $A_1$  and  $A_2$  in Fig. 1). Then, the four latest vertices will be on the lines tangent to the circle of  $b$  in diameter and parallel to this line  $A_1A_2$ . To avoid regular hexagons, these vertices are chosen in a random way between the two extremal cases which are on one hand the point located on the large circle (point  $P_1$  in Fig. 1) and on the other hand the point such as the small circle is the inscribed circle (point  $P_2$  in Fig. 1). In this work, we studied five different values of the elongation ratio:  $\frac{b}{a} = 1$  (circular particle); 0.8; 0.7; 0.6 and 0.5. The most elongated hexagons have thus their largest dimension twice the smallest one.

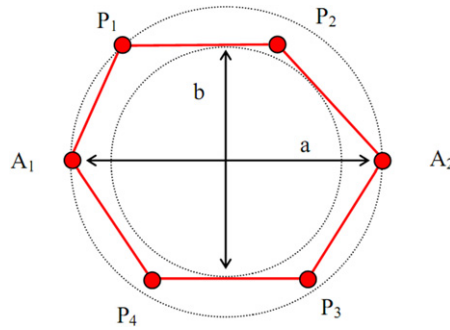


Fig. 1. Construction of an irregular hexagonal shape with an elongation ratio  $\frac{b}{a}$ .

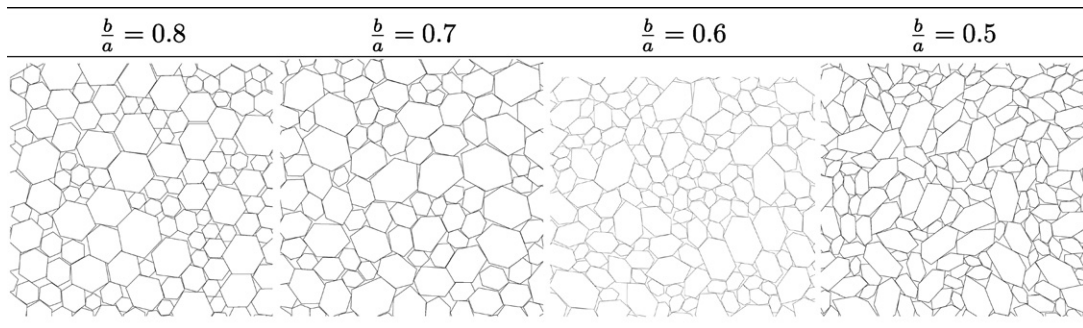


Fig. 2. Zoom in the assemblies made of elongated hexagons at the initial state.

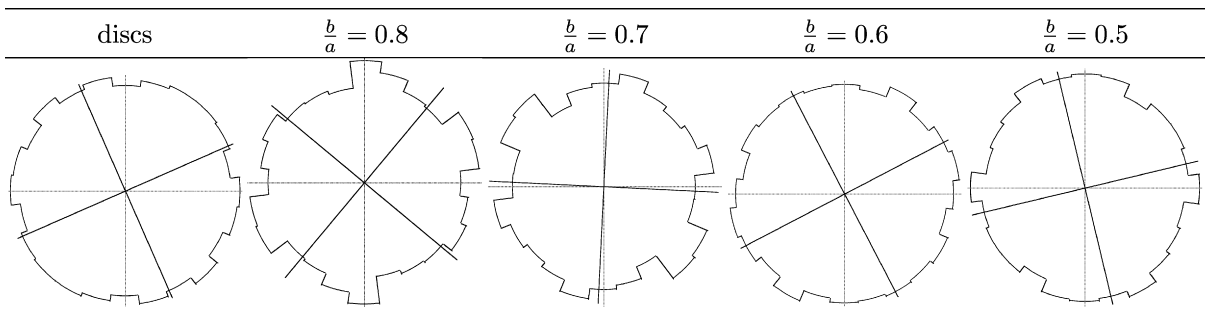


Fig. 3. Polar distributions of normal vector orientation in the initial configuration for every elongation ratio.

The granular sample is contained inside a box with rigid walls and the grains are perfectly rigid in these numerical simulations. Since each sample is made of grains with different shapes, we used a sample creation leading to the densest state (maximal relative density). First, a sample of non-contacting discs is generated with the particle size distribution chosen and they are then replaced by hexagons so that  $a = 2r$ . The hexagons are set with a random orientation, a random velocity and normal and tangential coefficients of restitution equal to 1 in order to have chocks without energy dissipation. The gravity and the coefficients of friction  $\mu_g$  between grains and  $\mu_w$  between walls and particles are set to zero. The sample is isotropically compressed with the same constant velocity applied to the top and the right walls. To avoid a looser area in the centre of sample, this displacement is regularly stopped so that the particles are evenly distributed inside the box, before pursuing the compression until a state of isotropic stress is reached. Five different samples with 4995 grains are generated: four of them are made of hexagons and the last one is made of discs. Fig. 2 shows zoom in samples for every assembly generated with the polygonal shapes. This generation procedure allows one to obtain homogeneous samples in respect to the density and to avoid a preferential direction of contact normal (Fig. 3), that would happen if the particles were deposited in the gravity field, especially in that case of elongated particles [17,32]. Moreover, it was also verified that the orientation of particles was randomly distributed: Fig. 4 shows the polar distributions of the hexagons' largest axis orientations.

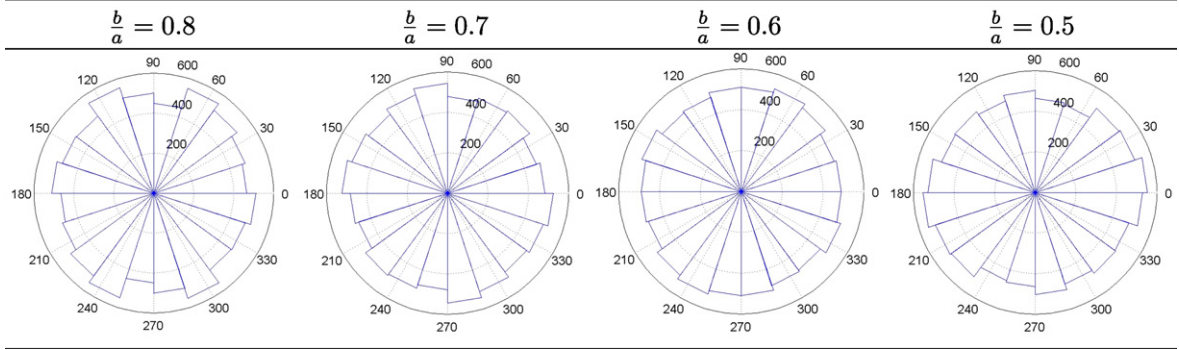


Fig. 4. Polar distributions of hexagon orientations in the initial configuration for every elongation ratio.

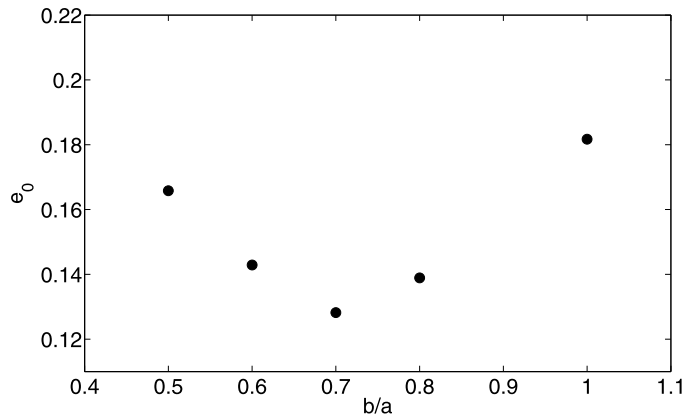


Fig. 5. Initial void ratio  $e_0$  as a function of the elongation ratio  $\frac{b}{a}$ .

### 3. Results

#### 3.1. Analysis of initial states

Fig. 5 shows the effect of grain elongation on the initial void ratio  $e_0$ . We can note that, for the studied shapes, the sample made of discs ( $\frac{b}{a} = 1$ ) is the loosest sample, which is consistent with previous numerical studies about the effect of particle angularity [14,15]. When the particle shape slightly deviates from the circular shape ( $\frac{b}{a} = 0.8$ ), the initial void ratio decreases to reach a minimum for  $\frac{b}{a} = 0.7$ , which corresponds to an aspect ratio  $\frac{a}{b} \approx 1.5$ . It is the same result as [33–35] who obtained, experimentally and numerically, the densest packing for ellipsoids with an aspect ratio equal to 1.5. For lower elongation ratio, the initial void ratio increases. The angularity of polygons allows first to reach a denser initial state, but the particle elongation reduces this ability and for very elongated particles, a larger initial void ratio is expected, as observed by [32–34].

We can also remark in Figs. 3 and 4 that the samples made of hexagons with  $\frac{b}{a} = 0.8$  and  $\frac{b}{a} = 0.7$  present distributions of contact directions and particle orientations with more fluctuations, in spite of the isotropic procedure used to generate the samples. This is because these hexagons are almost regular and only very slightly elongated. So, during the sample preparation, they arrange themselves with face-to-face contacts having almost all the same orientation. As a consequence, these samples also exhibit a more variable orientation distribution. It would be interesting to generate samples containing more particles and to test the repeatability of specimen creation in order to see whether a preferential direction emerges.

#### 3.2. Mechanical behaviour in biaxial compression

The biaxial compression tests are performed for a constant confining stress  $\sigma_0 = 10$  kPa by applying a constant horizontal velocity  $V_1$  onto the right wall. To avoid dynamics effects, the velocity  $V_1$  is chosen such as the inertia parameter  $I$  defined from [36] is small enough:  $I = \dot{\epsilon} \sqrt{\frac{m}{\sigma_0}} \leq 10^{-3}$ . The coefficients of friction are set to 0.5 between particles and kept to zero between walls and particles. For these quasistatic simulations, the contact network slowly evolves, so the restitution coefficients are decreased to  $e_N = 0.2$  and  $e_T = 0.1$ .

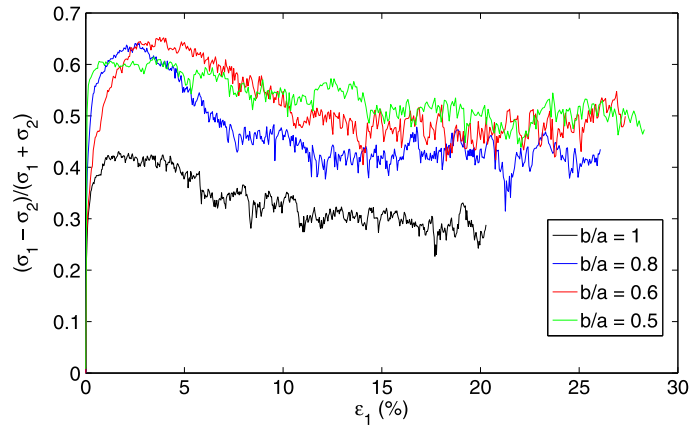


Fig. 6. Evolution of  $\frac{q}{p} = \frac{\sigma_1 - \sigma_2}{\sigma_1 + \sigma_2}$  as a function of the axial strain  $\epsilon_1$  for the sample of discs and 3 samples of elongated particles.

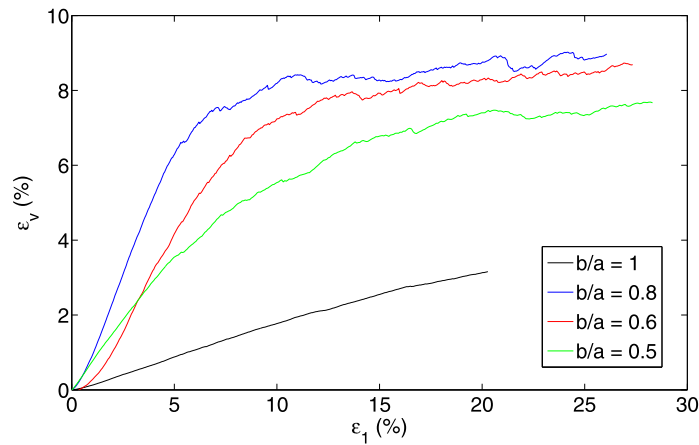


Fig. 7. Evolution of  $\epsilon_v$  as a function of the axial strain  $\epsilon_1$  for the sample of discs and 3 samples of elongated particles.

Figs. 6 and 7 show the stress–strain curves and the volumetric behaviour of samples during the biaxial compression. Since the samples are dense, the evolution of  $\frac{q}{p} = \frac{\sigma_1 - \sigma_2}{\sigma_1 + \sigma_2}$  as a function of the axial strain  $\epsilon_1$  exhibits a peak followed by a softening leading to a residual state. The sample of discs has a behaviour that is clearly different from the behaviour of samples with hexagons (black curve in Figs. 6 and 7): the shear resistance is greater for the samples made of non-circular particles. Angularity and particle elongation allow a better mobilisation of friction at contacts and restrict grain rotation, as it will be shown in the following section.

The effect of elongation on the value of the internal friction angles at peak  $\Phi^{peak}$  and at the residual state  $\Phi^*$  is shown in Fig. 8, where  $\sin \Phi = \frac{\sigma_1 - \sigma_2}{\sigma_1 + \sigma_2}$ . The sample made of hexagons with  $\frac{b}{a} = 0.7$  exhibits the larger  $\Phi^{peak}$  value, that can be connected with the fact that it is also the densest sample. Then  $\Phi^{peak}$  decreases with  $\frac{b}{a}$ . We observe a linear increase of the internal friction angle at the residual state  $\Phi^*$  in the range of the particle elongation examined here. The same result was observed by Ng [35] for samples made of ellipsoids with similar aspect ratios. In our study, the procedure chosen to generate the hexagons does not allow us to model particles with  $\frac{b}{a}$  greater than 0.8. So we cannot predict the evolution of  $\Phi^*$  and  $\Phi^{peak}$  for samples composed of particles whose shape gradually approaches a circular one. On the other hand, it would be interesting to simulate samples with more elongated particles ( $\frac{b}{a} < 0.5$ ) to check whether the linear increase of  $\Phi^*$  is confirmed or whether there is a value of  $\frac{b}{a}$  from which it no longer increases.

#### 4. Discussion

Many of the results found in the previous section can be explained by the particle angularity allowing them to exhibit face-to-face contacts. At the initial state, the samples made of polygonal particles are denser because this angular shape is able to better fill up the voids than the circular one. But beyond the elongation ratio  $\frac{b}{a} = 0.7$  these face-to-face contacts are less and less possible (there are 15% of face-to-face contacts in the sample with  $\frac{b}{a} = 0.8$ , whereas there are only 10% in the

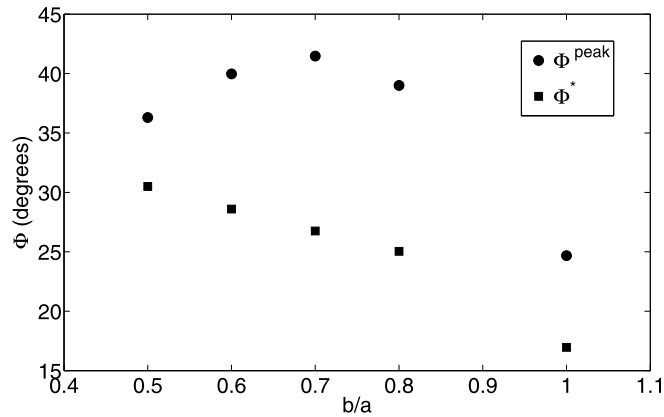


Fig. 8. Effect of the elongation ratio  $\frac{b}{a}$  on the friction angle at peak  $\phi^{\text{peak}}$  and at the residual state  $\phi^*$ .

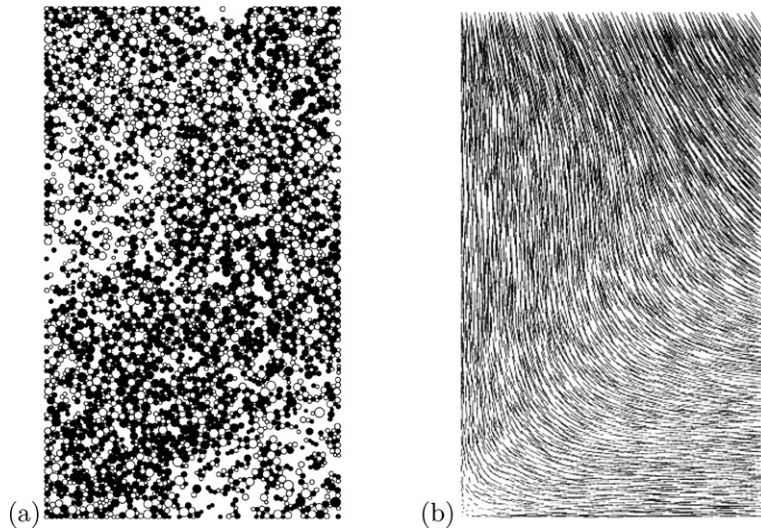
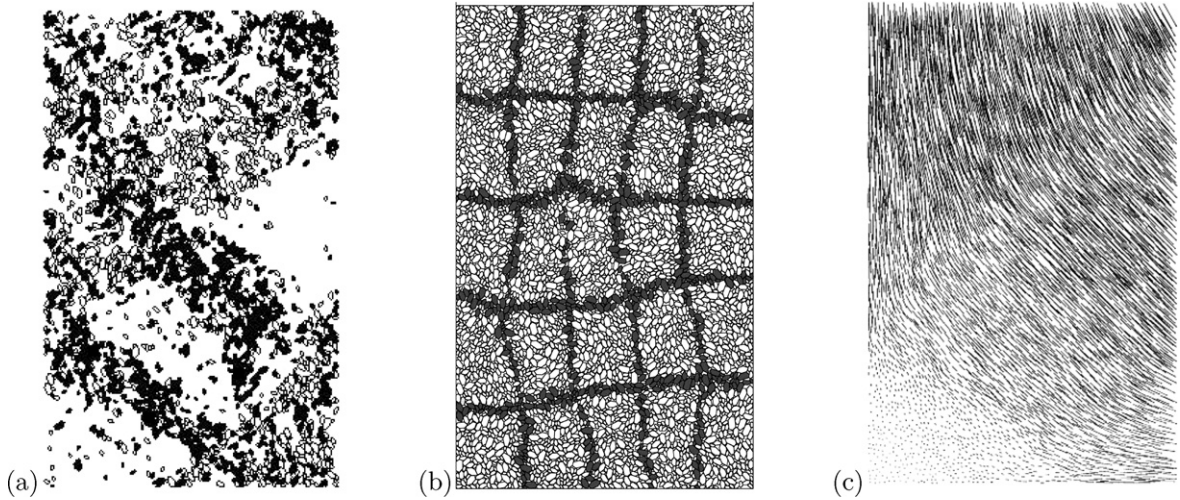


Fig. 9. (a) Cumulative rotation of discs from initial state to  $\varepsilon_1 = 20\%$ . The discs which rotate more than  $15^\circ$  anticlockwise are filled in black and respectively in white if it is a clockwise rotation. (b) Relative displacement of discs from initial state to  $\varepsilon_1 = 20\%$  showing the location of zones associated to large displacements.

sample with  $\frac{b}{a} = 0.5$ ) because the prevailing mechanism is the volume exclusion while it is negligible for a small deviation from the circular shape [37]. So, the initial void ratio increases for the samples made of the most elongated hexagons.

This ability for the angular particles to have face-to-face contacts also restricts the grain rotation during the biaxial compression. For the sample of discs, 77% of grains have a cumulative rotation (from the initial state to  $\varepsilon_1 = 20\%$ ) greater than  $\pm 15^\circ$ , while less than 50% of hexagons rotate more than  $15^\circ$  in absolute value for the same axial strain  $\varepsilon_1$ , whatever their elongation ratio. Moreover, these large rotations are not distributed in the same way for the discs than for the polygons: large rotations are uniformly distributed inside the sample of discs (Fig. 9) but are located along thin bands for the samples of hexagons (Fig. 10). This phenomenon is linked with the width and persistence of shear bands, which is not the same in samples of discs and samples of polygons. They are more spread in the case of circular particles and are very volatile. In Fig. 11 the large cumulative rotation of discs is shown for strain increments of 5%. One can see that zones where the cumulative rotation is large move depending on the strain amplitude. On the contrary for samples made of angular grains, shear bands are thinner [38] and they change very little during the deformation, as shown in Fig. 12. This is consistent with the result obtained in [2,39] and [40], where numerical simulations were performed on samples of discs, but by introducing some rolling resistance at contact points in order to reproduce a high gradient of particle rotation along the shear band, as is found in actual sand. Finally, we can note that for these hexagonal particles, the rotations have the same direction inside a given shear band (anticlockwise or clockwise), this confirms the importance of sliding contacts (increasing the mobilisation of friction) for these elongated shapes.



**Fig. 10.** (a) Cumulative rotation of hexagons with  $\frac{b}{a} = 0.5$  from initial state to  $\varepsilon_1 = 20\%$ . The grains which rotate more than  $15^\circ$  anticlockwise are filled in black and respectively in white if it is a clockwise rotation. (b) Deformation after  $\varepsilon_1 = 20\%$  of an initial regular grid imprint on the sample of hexagons with  $\frac{b}{a} = 0.5$  at the initial state, showing the location of the most distorted zones. (c) Relative displacement of hexagons with  $\frac{b}{a} = 0.5$  from initial state to  $\varepsilon_1 = 20\%$  showing the location of zones associated to large displacements. The cases of hexagons with  $\frac{b}{a} > 0.5$  are similar.

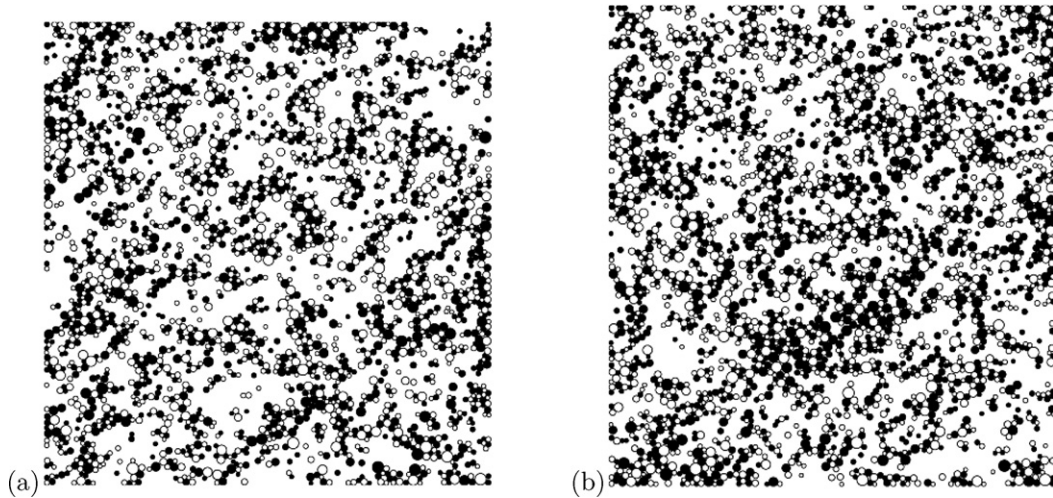


**Fig. 11.** Cumulative rotation of discs (a) from initial state to  $\varepsilon_1 = 5\%$  and (b) from  $\varepsilon_1 = 5\%$  to  $\varepsilon_1 = 10\%$ . The grains which rotate more than  $5^\circ$  anticlockwise are filled in black and respectively in white if it is a clockwise rotation.

## 5. Conclusions and perspectives

Numerical simulations of biaxial compression were performed on samples composed of either hexagons or discs in order to analyse the effect of particle angularity and elongation. The mechanical response of these samples was analysed in particular in comparison to that of a sample of circular particles. Our results show that particle shapes modify the global and local behaviours of these granular materials.

- For the range of  $\frac{b}{a}$  ratio studied and for the same initial confining pressure, the samples made of angular particles are denser than the sample made of circular particles, but the particle elongation reduces this ability and density of samples with hexagons decreases with their elongation.
- Samples made of angular particles exhibit larger shear strength and dilatancy due to the face-to-face contacts that restrict rotations and the friction angle at the residual state is found to linearly increase with the particle elongation, for the range of  $\frac{b}{a}$  ratio studied.
- The large rotations are distributed inside the whole sample of discs whereas they are located inside thin bands for the samples made of angular grains, because the shear bands are thinner and more persistent in these media.

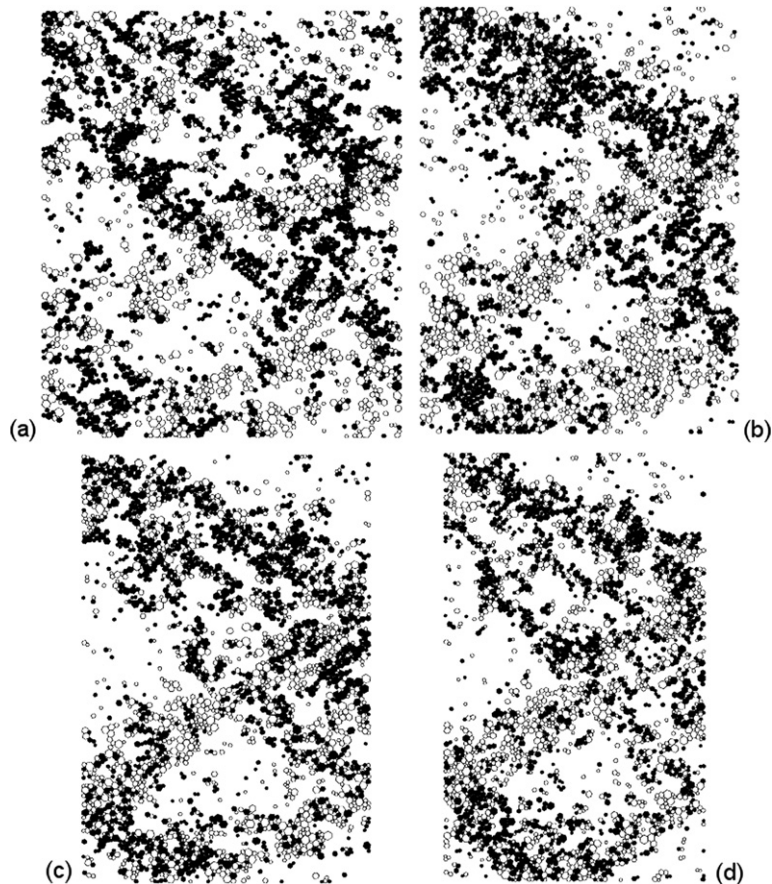


**Fig. 12.** Cumulative rotation of hexagons with  $\frac{b}{a} = 0.2$ , (a) from initial state to  $\varepsilon_1 = 5\%$ , (b) from  $\varepsilon_1 = 5\%$  to  $\varepsilon_1 = 10\%$ , (c) from  $\varepsilon_1 = 10\%$  to  $\varepsilon_1 = 15\%$  and (d) from  $\varepsilon_1 = 15\%$  to  $\varepsilon_1 = 20\%$ . The grains which rotate more than  $5^\circ$  anticlockwise are filled in black and respectively in white if it is a clockwise rotation.

Therefore, DEM simulations using only circular or spherical particles seem too restrictive. If the introduction of rolling resistance is an attractive solution [39,40], the difficulty of this strategy lies in choosing the value of such a parameter. Taking into account the non-circular shape of the particles (angularity and elongation) allows to introduce into the numerical model only parameters whose physical origin is clear.

Further analyses are presently under way in order to correlate these results with the evolution of some local parameters (coordination number, anisotropy of contact forces) and to clarify the effect of particle elongation. Comparisons with the results obtained for samples made of some other shapes (octagons [41], clumps made of overlapping discs [42,43], rectangles with rounded caps [37], etc.) are also in progress, in order to extend this analysis and to generalise the effect of the grain shape on the mechanical behaviour of granular materials.

### Acknowledgement

This work is a part of the CEGEO program, a French national research project.

### References

- [1] M. Oda, K. Iwashita, *Mechanics of Granular Materials: An Introduction*, Balkema, Rotterdam/Brookfield, 1999.
- [2] M.R. Kuhn, Structured deformation in granular materials, *Mech. Mater.* 31 (1999) 407–429.
- [3] M. Lätzel, S. Luding, H.J. Herrmann, Macroscopic material properties from quasi-static, microscopic simulations of a two-dimensional shear-cell, *Gran. Matter* 2 (2000) 123–135.
- [4] L. Rothenburg, N.P. Kruyt, Critical state and evolution of coordination number in simulated granular materials, *Int. J. Solids Struct.* 41 (2004) 5763–5774.
- [5] M. Lätzel, S. Luding, H.J. Herrmann, D.W. Howell, R.P. Behringer, Comparing simulation and experiment of a 2D granular Couette shear device, *Eur. Phys. J. E* 11 (2003) 325–333.
- [6] S. Luding, Micro–macro transition for anisotropic, frictional granular packings, *Int. J. Solids Struct.* 41 (2004) 5821–5836.
- [7] P.W. Cleary, The effect of particle shape on hopper discharge, in: *Proceedings of the Second International Conference of the CFD in the Minerals and Process Industries*, Melbourne, Australia, 6–8 December 1999.
- [8] P.W. Cleary, M.L. Sawley, DEM modelling of industrial granular flows: 3D case studies and the effect of particle shape on hopper discharge, *Appl. Math. Model.* 26 (2002) 89–111.



- [9] P. Guo, X. Su, Shear strength, interparticle locking, and dilatancy of granular materials, *Can. Geotech. J.* 44 (5) (2007) 579–591.
- [10] A. Tsomokos, V.N. Georgiannou, Effect of grain shape and angularity on the undrained response of fine sands, *Can. Geotech. J.* 47 (2010) 539–551.
- [11] L. Rothenburg, R.J. Bathurst, Micromechanical features of granular assemblies with planar elliptical particles, *Géotechnique* 42 (1992) 79–95.
- [12] H.-G. Matuttis, S. Luding, H.J. Herrmann, Discrete element methods for the simulation of dense packings and heaps made of spherical and non-spherical particles, *Powder Technol.* 109 (2000) 278–292.
- [13] S. Antony, M. Kuhn, Influence of particle shape on the interplay between contact signatures and particulate strength, *Int. J. Solids Struct.* 41 (2004) 5863–5870.
- [14] A.A. Mirghasemi, L. Rothenburg, E.L. Matyas, Influence of particle shape on engineering properties of assemblies of two-dimensional polygonal-shaped particles, *Géotechnique* 52 (3) (2002) 209–217.
- [15] E. Azéma, F. Radjai, R. Peyroux, G. Saussine, Force transmission in a packing of pentagonal particles, *Phys. Rev. E* 76 (2007) 011301.
- [16] C. Nouguier-Lehon, B. Cambou, E. Vincens, Influence of particle shape and angularity on the behaviour of granular materials: A numerical analysis, *Int. J. Numer. Anal. Meth. Geomech.* 27 (2003) 1207–1226.
- [17] C. Nouguier-Lehon, E. Vincens, B. Cambou, Structural changes in granular materials: The case of irregular polygonal particles, *Int. J. Solids Struct.* 42 (2005) 6356–6375.
- [18] A.A. Peña, R. García-Rojo, H.J. Herrmann, Influence of particle shape on sheared dense granular media, *Gran. Matter* 9 (2007) 279–291.
- [19] F. Alonso-Marroquín, S. Luding, H.J. Herrmann, I. Vardoulakis, Role of anisotropy in the elastoplastic response of a polygonal packing, *Phys. Rev. E* 71 (2005) 051304.
- [20] J.J. Moreau, Some numerical methods in multibody dynamics: Application to granular materials, *Eur. J. Mech. A/Solids* 13 (4-suppl.) (1994) 93–114.
- [21] M. Jean, The non-smooth contact dynamics method, *Comp. Meth. Appl. Mech. Eng.* 177 (1999) 235–257.
- [22] J.J. Moreau, Numerical aspects of the sweeping process, *Comp. Meth. Appl. Mech. Eng.* 177 (1999) 329–349.
- [23] F. Radjai, V. Richefeu, Contact Dynamics as a nonsmooth discrete element method, *Mech. Mater.* 41 (2009) 715–728.
- [24] P.A. Cundall, O.D.L. Strack, A discrete numerical model for granular assemblies, *Géotechnique* 29 (1979) 47–65.
- [25] G. Saussine, C. Cholet, P.E. Gautier, F. Dubois, C. Bohatier, J.J. Moreau, Modelling ballast behaviour under dynamic loading, Part 1: A 2D polygonal discrete element method approach, *Comp. Meth. Appl. Mech. Eng.* 195 (2005) 19–22.
- [26] A. Taboada, N. Estrada, Rock-soil avalanches: Theory and simulation, *J. Geophys. Res.* 114 (2009) F03004.
- [27] B. Chetouane, F. Dubois, M. Vinches, C. Bohatier, NSCD discrete element method for modelling masonry structures, *Int. J. Num. Meth. Eng.* 64 (2005) 65–94.
- [28] B. Maurin, P. Cañadas, H. Baudriller, P. Montcourrier, N. Bettache, Mechanical model of cytoskeleton structuration during cell adhesion and spreading, *J. Biomechanics* 41 (2008) 2036–2041.
- [29] C. Nouguier-Lehon, P. Dubujet, B. Cambou, Analysis of granular material behaviour from two kinds of numerical modelling, in: *Proceedings of the 15th ASCE Engineering Mechanics Conference*, Columbia University, New York, 2002.
- [30] D. Kadau, D. Schwesig, J. Theuerkauf, D.E. Wolf, Influence of particle elasticity in shear testers, *Gran. Matter* 8 (2006) 35–40.
- [31] J.K. Mitchell, K. Soga, *Fundamentals of Soil Behavior*, 3rd ed., Wiley, 2005.
- [32] R. Cruz Hidalgo, I. Zuriguel, D. Maza, I. Pagonabarraga, Granular packings of elongated faceted particles deposited under gravity, *J. Stat. Mech.* (2010) P06025.
- [33] A. Donev, F.H. Stillinger, P.M. Chaikin, S. Torquato, Unusually dense crystal packings of ellipsoids, *Phys. Rev. Lett.* 92 (2004) 255506.
- [34] A. Donev, R. Connelly, F.H. Stillinger, S. Torquato, Underconstrained jammed packings of nonspherical hard particles: Ellipses and ellipsoids, *Phys. Rev. E* 75 (2007) 051304.
- [35] T.-T. Ng, Particle shape effect on macro- and micro-behaviors of monodisperse ellipsoids, *Int. J. Numer. Anal. Meth. Geomech.* 33 (2009) 511–527.
- [36] G.D.R. MiDi, On dense granular flows, *Eur. Phys. J. E* 14 (2004) 341–365.
- [37] E. Azéma, F. Radjai, Stress-strain behavior and geometrical properties of packing of elongated particles, *Phys. Rev. E* 81 (2010) 051304.
- [38] E. Gerolymatou, F. Froio, C. Nouguier-Lehon, Energy-rates for granular materials: Discrete characterization, in: *Proceedings of the 9th International Congress on Mechanics*, Limassol, Cyprus, 12–14 July 2010.
- [39] K. Iwashita, M. Oda, Micro-deformation mechanism of shear banding process based on modified distinct element method, *Powder Technol.* 109 (2000) 192–205.
- [40] A. Mohamed, M. Gutierrez, Comprehensive study of the effects of rolling resistance on the stress-strain and strain localization behavior of granular materials, *Gran. Matter* 12 (5) (2010) 527–541. Special Issue: IS-Shanghai 2010: International Symposium on Geomechanics and Geotechnics: From Micro to Macro, Shanghai, China, October 2010/Guest Edited by Mingjing Jiang and Fang Liu.
- [41] M. Chaze, Effect of grain shape on the behaviour of granular materials in biaxial compression, in: *COMGEO Conference*, Juan-les-Pins, 29 April–1 May, 2009.
- [42] B. Saint-Cyr, C. Voivret, J.-Y. Delenne, F. Radjai, P. Sornay, Effect of shape nonconvexity on the shear strength of granular media, in: M. Nakagawa, S. Luding (Eds.), *Proceedings of Powders and Grains Conference*, 13–17 July 2009, Golden, USA, pp. 389–392.
- [43] K. Szarf, G. Combe, P. Villard, Influence of the grains shape on the mechanical behavior of granular materials, in: M. Nakagawa, S. Luding (Eds.), *Proceedings of Powders and Grains Conference*, 13–17 July 2009, Golden, USA, pp. 357–360.